Supplemental Figure 1. Sample line profile data for 67NR and 4T1 tumours from the radiography images displayed in Figure 2.

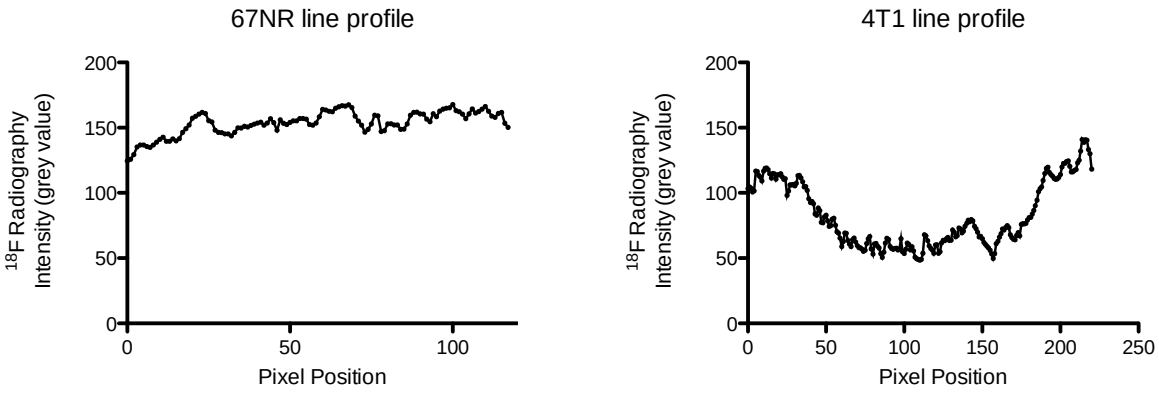

Supplemental Figure 2. (A) Cumulative frequency plots of static PET scans conducted 55 minutes post-injection of 2-^{18}F-FEtOH. Data display that 4T1 tumours voxel intensities are shifted left towards reduced radioactivity detected. This is quantified in (B) by comparing the 50th and 90th percentiles, both of which are significantly lower activity in 4T1 tumours.

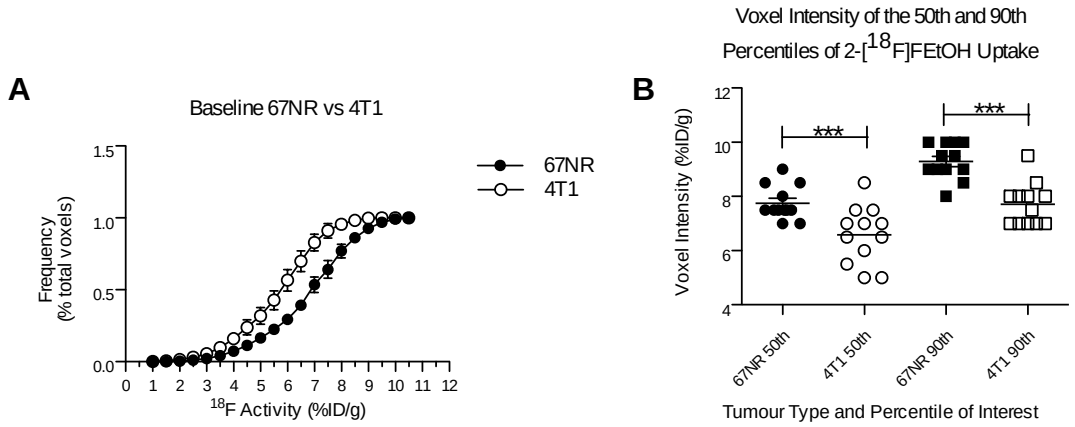

Supplemental Figure 3. Image derived input functions were produced based on the voxels within the Vena Cava, identified during the first pass of the 2-^{18}F-FEtOH bolus after the tail vein injection. Displayed is the input function averaged across four dynamic scans from untreated mice. Data points were produced every 5 seconds across the first 2 minutes, then every 30 seconds up until 5 minutes post-injection, and finally every 5 minutes until the end of the 60 minute PET scan.

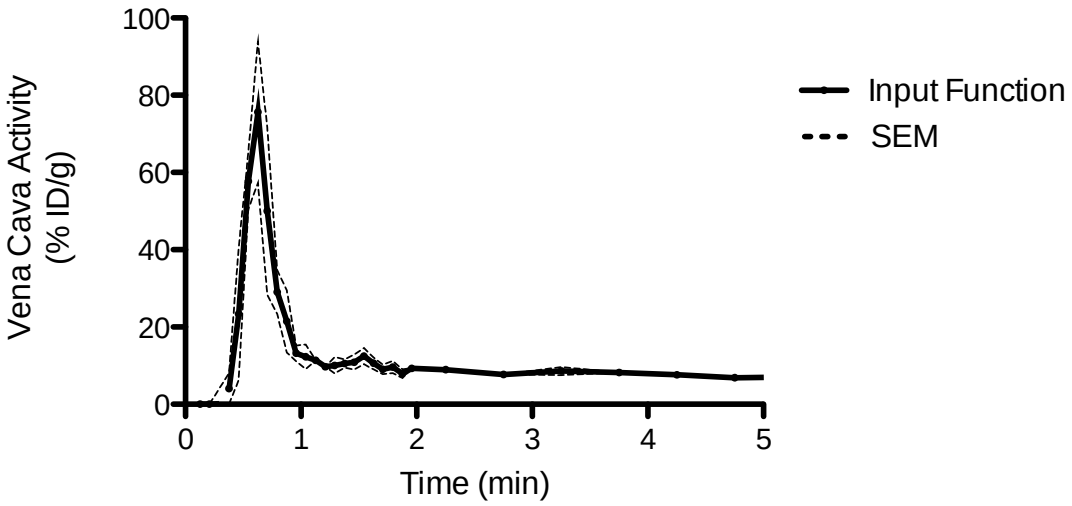

Supplemental Figure 4. Pentoxifylline shifted 4T1 (A) and 67NR (B) 2-^{18}F-FEtOH radiography histograms towards increased radioactivity, consistent with the understood effect of pentoxifylline to increase tumour perfusion.

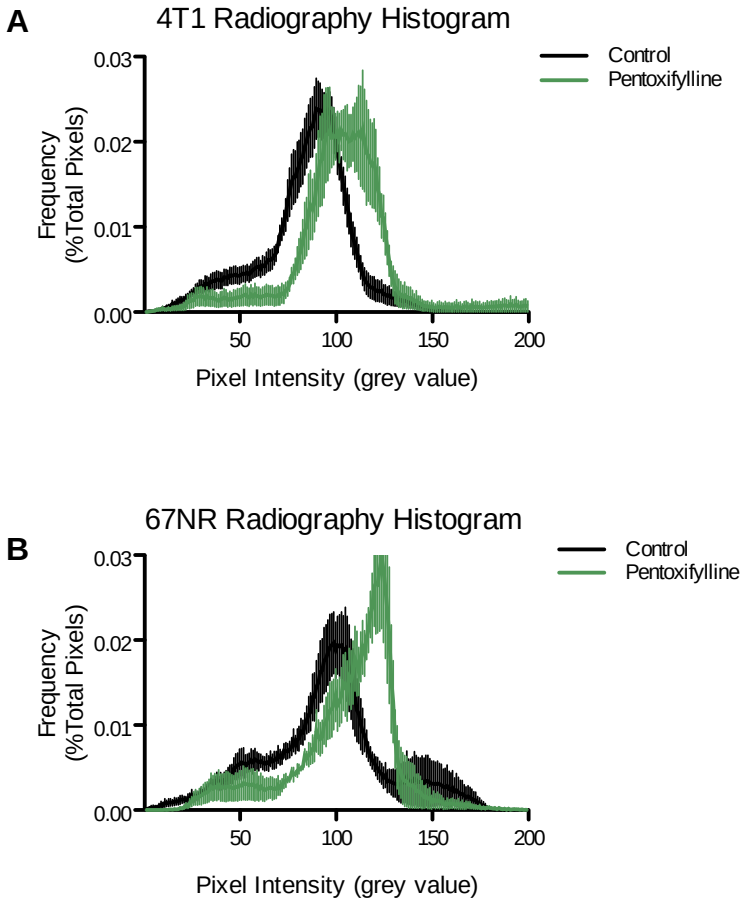

Supplemental Figure 5. Representative images from dynamic PET scans of the same mouse imaged for untreated baseline images (A) on the first day, and hydralazine pre-treatment (B). Images left to right are 1 minute post-injection of 2-^{18}F-FEtOH, 10 minutes post-injection, and 55 minutes post-injection.

A

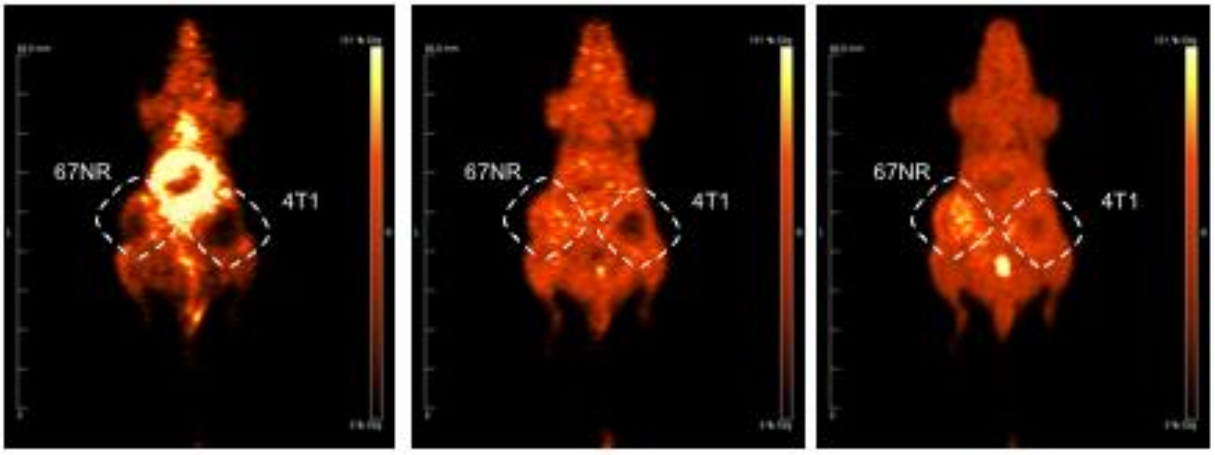

B

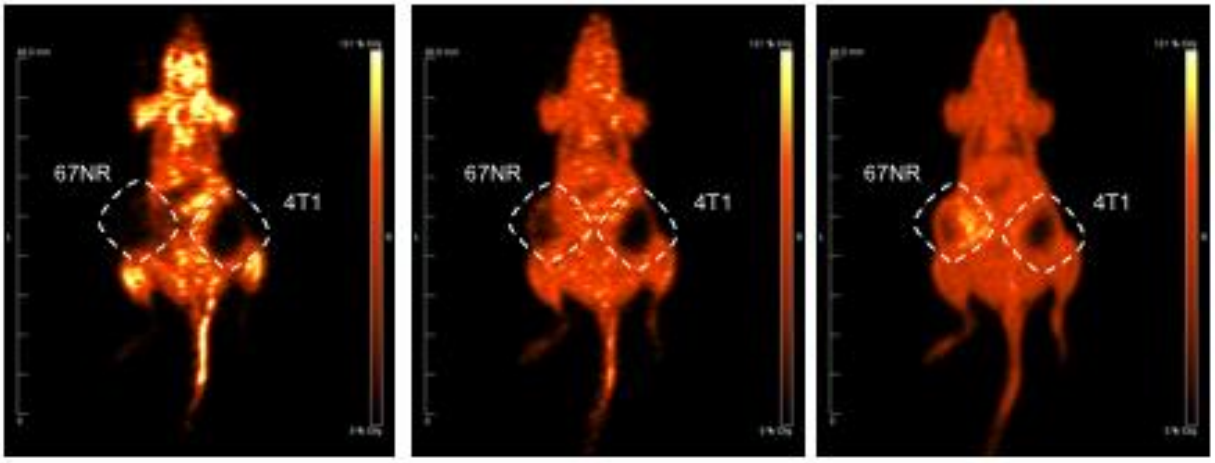

Supplemental Figure 6. Hydralazine induces an increase in skeletal muscle 2-^{18}F-FEtOH activity consistent with the 'steal effect'. Further, we observed a complete inhibition of 2-^{18}F-FEtOH clearance to the bladder in hydralazine treated mice, consistent with the fluid-retention effect of hydralazine.